Phase Aberrations in Diffraction Microscopy

S. Marchesini[1,4], H. N. Chapman[1,4], A. Barty[1], M. R. Howells[2], J. C. H. Spence[3,2], C. Cui[2], U. Weierstall[3], and A. M. Minor[5]

[1]University of California, Lawrence Livermore National Laboratory, 7000 East Ave. Livermore CA 94550, USA
[2]Advanced Light Source, Lawrence Berkeley National Laboratory, 1 Cyclotron Road, Berkeley, CA 94720, USA
[3]Department of Physics and Astronomy, Arizona State University, Tempe, AZ 85287-1504, USA
[4]Center for Biophotonics Science and Technology, UC Davis, 2700 Stockton Blvd., Suite 1400, Sacramento CA 95817, USA
[5]National Center for Electron Microscopy, Lawrence Berkeley National Laboratory, 1 Cyclotron Road, Berkeley, CA 94720, USA

In coherent X-ray diffraction microscopy the diffraction pattern generated by a sample illuminated with coherent x-rays is recorded, and a computer algorithm recovers the unmeasured phases to synthesize an image. By avoiding the use of a lens the resolution is limited, in principle, only by the largest scattering angles recorded. However, the imaging task is shifted from the experiment to the computer, and the algorithm's ability to recover meaningful images in the presence of noise and limited prior knowledge may produce aberrations in the reconstructed image. We analyze the low order aberrations produced by our phase retrieval algorithms. We present two methods to improve the accuracy and stability of reconstructions.

KEYWORDS: Coherent diffraction, X-ray microscopy, Phase retrieval, Lensless Imaging

1. Introduction

A new imaging technique has emerged in recent years that can overcome many limitations of light, electron, and X-ray microscopy. Coherent X-ray Diffraction Microscopy (CXDM) [1] promises to enable the study of thick objects at high resolution. In this technique one records the 3D diffraction pattern generated by a sample illuminated with coherent x-rays, and as in x-ray crystallography a computer recovers the unmeasured phases. This is done by alternately applying constraints such as the measured intensity in reciprocal space and the object support—the region where the object is assumed to be different from 0—in real space. This corresponds to defining the envelope of a molecule in crystallography. In our implementation the support is periodically updated based on the current object estimate[2].

By avoiding the use of a lens, the experimental requirements are greatly reduced, and the resolution becomes limited only by the radiation damage [3,4]. However the imaging task is shifted from the experiment to the computer, and the technique may be limited by our understanding of the phase recovery process as well as the algorithm's ability to recover meaningful images in the presence of noise and limited prior knowledge.

Recently we have presented experimental results of high-resolution 3D X-ray diffraction imaging of a well-characterized test object to demonstrate the practical application of these advances [5,6]. Here we extend the analyis of image reconstruction and determine low-order phase errors (essentially image aberrations) that can occur when reconstructing general complex-valued images. We present two methods to improve the accuracy and stability of reconstructions.

2. Coherent X-Ray Diffraction

Three-dimensional coherent X-ray diffraction data were collected at the Advanced Light Source [7,8] from a test object that consisted of 50-nm diameter gold spheres located on a 2.5-µm-wide silicon nitride pyramid [5] (Fig. 1a). A bare CCD located in the far field recorded the diffraction patterns with a pixel sampling that was more than 4 times the Shannon sampling rate for the (phased) complex amplitudes. Diffraction patterns were collected for many sample orientations over an angular range of 129°. These were interpolated onto a 3D grid. We reconstructed a full 3D image by performing phase retrieval on the entire 3D diffraction dataset (i.e. the iterations involved three-dimensional FFTs). The resulting volume image reveals the structure of the object in all three dimensions and can be visualized in many ways including projections through the data, slices (tomographs), or isosurface rendering of the data.

In addition to 3D images, we perform much analysis and algorithm development on 2D datasets. For the work in this paper we choose central plane sections extracted from the 3D diffraction pattern. By the Fourier projection theorem, the image formed from a central section is an infinite depth-of-focus projection image (Fig. 1b). We carry out *ab initio* image reconstructions using the Relaxed Averaged Alternating Reflections (RAAR) algorithm [9] with the "Shrinkwrap" dynamic support constraint [2]. Details of the algorithm parameters used are given in Chapman [5].

3. Resolution Analysis

The phase retrieval process recovers the diffraction phases with limited accuracy, due to factors including SNR of the diffraction amplitudes, missing data, the inconsistency of constraints, and systematic errors in the data (such as errors in interpolation). These errors in phase reduce the resolution of the synthesized image. With a complex image a loose support constraint will lead to unconstrained low-order aberrations. As is well known an object could be shifted by a few pixels each time we reconstruct, which is equivalent to a varying linear phase ramp in reciprocal space. In addition to this shift low order phase variations, such as defocus and astigmatism can also be unconstrained if the aberrated object fits inside the support. One way to quantify the effect of
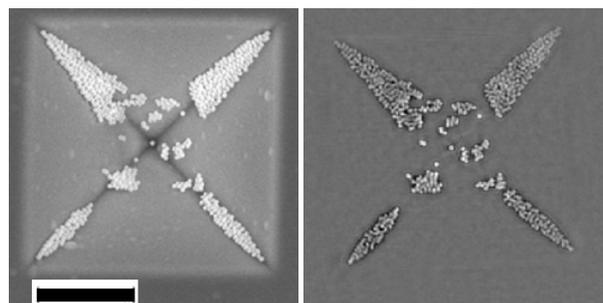

Fig. 1. (a) SEM image of the 3D test object. Scalebar is 1 micron. (b) Infinite depth-of-focus image reconstructed from a central section of the 3D coherent X-ray diffraction data.
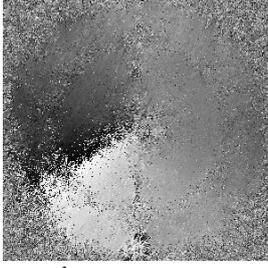
Fig. 2. Phase difference between two reconstructions in reciprocal space, showing a phase vortex between two solutions in the far field. The center of the vortex is at $q = 0$, and the half-width of the phase map is $q = 0.048$ nm^{-1}.

these phase variations is to determine the variation in retrieved phases as a function of resolution [10]. Given a reconstructed image $g(x)$ obtained by phase retrieval starting from random phases, and its Fourier transform $G = |G| \exp\{i\varphi(q)\}$, we define the phase retrieval transfer function by

$$\text{PRTF}(\mathbf{q}) = \left| \left\langle \exp\{i\varphi(\mathbf{q})\} \right\rangle \right| = \left| \left\langle \frac{G(\mathbf{q})}{|G(\mathbf{q})|} \right\rangle \right| \qquad (1)$$

with $\langle G \rangle$ the average over the complex diffraction amplitudes of many reconstructed images starting from random phases. Where the phases are random and completely uncorrelated, the average will approach zero. Thus, the ratio is effectively a transfer function for the phase retrieval process, and the average image (the Fourier tranform of $\langle G \rangle$) is the best estimate of the image: spatial frequencies are weighted by the confidence in which their phases are known.

In our case when reconstructing complex 2D images, with low frequencies missing due to the beamstop, we have observed that phase retrieval from independent random starts may differ by a phase vortex (right or left handed), centered at the zero spatial frequency (Fig. 2). We find that we can improve the estimate of the image by separating out the vortex modes [5]. These phase vortices are due to stagnation of the phase retrieval process. Other phase vortices can appear near local minima of the measured intensities, and our method of separating solutions will fail to detect vortices not centered near the beamstop. In order to remove these vortex aberrations we modified the reconstruction algorithm as follows: (i) Average n independent reconstructions which will likely average out the phase vortex modes but will also smooth the resulting image, reducing the resolution. (ii) Refine this averaged image by inputting it to the RAAR [8] algorithm and carrying out 200 iterations. Using this "averaged RAAR" algorithm we reduced the probability of recovering an image with phase vortex mode from 40% to 15%, resulting in an improvement of the PRTF by almost a factor of two.

We compute the final image, and the PRTF, by averaging 1000 such reconstructions (Fig. 3). Before averaging many images we make sure that they are not shifted with respect to one another by finding the linear phase ramp that minimizes the difference between their Fourier transforms. Fluctuations of the linear phase term indicate fluctuations in positions. Fluctuations in higher order polynomial phase terms indicate that phase aberrations are present in the reconstructions.
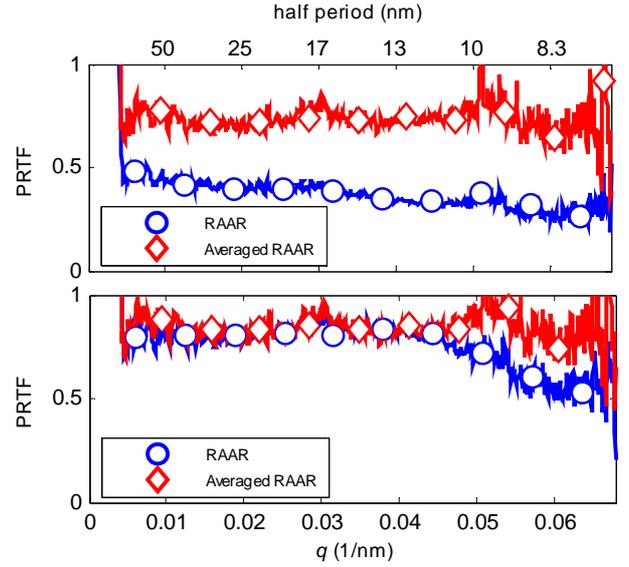

Fig. 3. Top: Phase retrieval transfer function of the two algorithms. PRTF=1 represents stable phases. The averaged RAAR algorithm significantly improves the stability of the reconstructions. Bottom: PRTF after removing the vortices centered at $q = 0$. The averaged RAAR shows marked improvements at high frequencies.

To quantify the instabilities of these low order phase modes, we find the low order phase modes (focus, astigmatism, coma, up to a polynomial of order n_p) that minimize the difference between each new reconstruction G_n and the first recovered image G_0. This is done by minimizing

$$\chi = \sum_{\mathbf{q}} \left| G_0(\mathbf{q}) - G_n(\mathbf{q}) \exp\{ip(\mathbf{q})\} \right|^2 \qquad (2)$$

with the 2D polynomial defined by coefficients $p_{i,j}$ as

$$p(\mathbf{q}) = \sum_{i,j=0}^{i+j \le n_p} p_{i,j}\, \bar{q}_x^i\, \bar{q}_y^j \qquad (3)$$

with $\bar{q}_{x,y} = q_{x,y} / 2\max(q_{x,y})$. The linear terms representing shifts in real space are found using the method described by Fienup [11], while higher order terms are obtained by fitting the phase difference, $\arg(G_0^\dagger G_n)$, to the higher order 2D polynomial terms and iterating until the correction is less than 1°. The fluctuations of the second order polynomial coefficients are obtained by calculating their standard deviation among 1000 reconstructions, and we find that

$$\text{std}\begin{pmatrix} p_{0,0} & p_{1,0} & p_{2,0} \\ p_{0,1} & p_{1,1} & p_{2,1} \\ p_{0,2} & p_{1,2} & p_{2,2} \end{pmatrix} = \begin{pmatrix} 2.26 & 0.31 & 0.15 \\ 0.53 & 0.61 & 0 \\ 0.14 & 0 & 0 \end{pmatrix} \qquad (4)$$

The linear terms $(p_{1,0}\ p_{0,1})$ represent a shift of $[0.31, 0.53]/2\pi = [0.049, 0.085]$ pixels in real space corresponding to 0.5 and 0.8 nm shifts in x and y. The degree of defocus phase variation depends on $(p_{2,0} + p_{0,2})/2$, and the real-space defocus variation is given by:

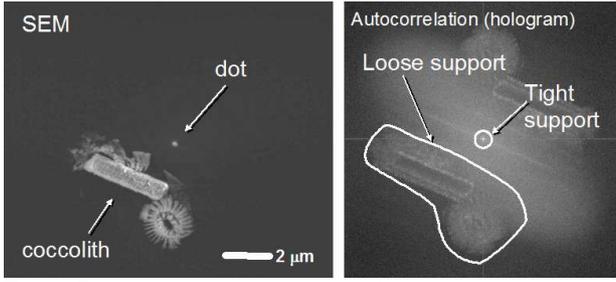$$\delta z = \frac{\lambda}{4\pi\, \text{NA}^2} \text{std}\{p_{2,0} + p_{0,2}\} \qquad (5)$$

Fig. 4. Demonstration of reference-enhanced diffraction imaging. A Pt dot was deposited near the sample (a coccolith) with a focused ion beam instrument. The Fourier transform of the diffraction intensities (right) can be used to determine the support which can constrain the low-order phase aberrations.
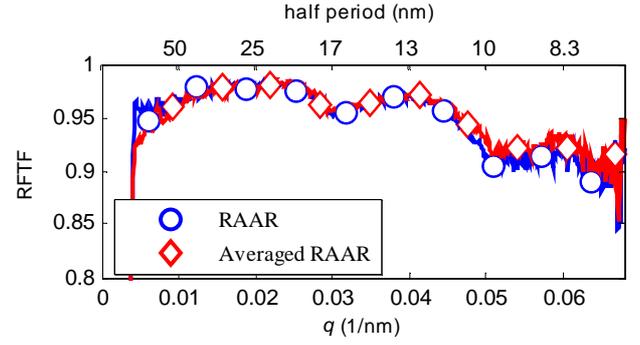

Fig. 5. The R-Factor Transfer Function (RFTF) of a reconstructed image, showing excellent agreement with the measured diffraction intensities.

We have NA=0.084 and λ=1.65 nm, giving $\delta z = 11.3$ nm. Note that this defocus variation represents an instability of the phase retrieval process and does not correspond to an optical effect of focusing through a thick object. In this case all voxels of the 3D images or pixels of the 2D projection images are equally aberrated by this effect.

An additional method to further reduce these instabilities is to use a small reference point near the specimen. During the retrieval process the image of the reference point is forced to be small with a tight support. This constrains the aberrations at this image point, and hence at all image points. The reference point has the additional advantage of providing a hologram of the specimen (Fig. 4) which can be used to provide the object support, or even the desired image.

To quantify our ability to recover unmeasured intensities (for example behind the beamstop) we use the normalized standard deviation

$$\sigma^2(\mathbf{q}) = \left\langle \left| G(\mathbf{q}) - \bar{G}(\mathbf{q}) \right|^2 \right\rangle \Big/ \left| \langle G(\mathbf{q}) \rangle \right|^2 . \quad (6)$$

We define a transfer function, based on σ^2 as:

$$\mathrm{TF}(\mathbf{q}) = \frac{1}{\sqrt{1 + \sigma^2(\mathbf{q})}} = \frac{|\langle G(\mathbf{q}) \rangle|}{\sqrt{\langle |G(\mathbf{q})|^2 \rangle}} \quad (7)$$

which has the desired properties that transfer function is unity for $\sigma^2 = 0$ and zero for $\sigma^2 = \infty$. Eqn. (7) reduces to the PRTF in the regions of $\mathbf{q}$ where $|G|$ is measured.

An algorithm that always recovers the same phases does not necessarily recover the correct ones. Another requirement is that the recovered image is constrained in the region called support: $g(x) = 0, x \notin S$. If this condition is satisfied the Fourier modulus condition ($|G| = I^{1/2}$) is unlikely to be satisfied in the presence of noise. We can quantify deviations from the measured values by an R-factor (similar to that used in crystallography[12]) by

$$\sigma_{RF}^2(\mathbf{q}) = \frac{\left\| G(\mathbf{q}) \right| - \sqrt{I}(\mathbf{q}) \right\|^2}{\left| \sqrt{I}(\mathbf{q}) \right|^2} \quad (8)$$

and its related transfer function $\mathrm{RFTF}(\mathbf{q}) = \left[1 + \sigma_{RF}^2(\mathbf{q}) \right]^{-1/2}$, which is plotted in Fig. 5 for a reconstructed image.

4. Conclusion

We have performed a characterization of high-resolution imaging of an isolated 3D object by *ab initio* phase retrieval of the coherent X-ray diffraction, and examined metrics to allow the quality of image reconstructions to be assessed.

The phase retrieval process does not produce unique images, in that varying low-order phase modes arise, akin to aberrations in an imaging system. Other than the tilt terms, the low-order phase aberrations discussed here will be reduced in case of a real object (for which only antisymmetric terms are allowed) and will not be present when a real-space positivity constraint can be imposed, since defocusing or otherwise aberrating an image causes it to be complex. However, in the case of samples consisting of more than one material (such as biological samples) the object cannot be considered positive and we must reduce the effects of aberrations. We have proposed two methods of overcoming limitations of computer reconstruction: in order to improve the stability of the reconstructions we average several reconstructed images and use the result to feed a new round of phase retrieval. From an experimental point of view, the use of a reference point, or other well-defined object, should enable us to greatly reduce low order phase aberrations.

1) J. Miao, C. Charalambous, J. Kirz, and D. Sayre, Nature, **400** (1999) 342.
2) S. Marchesini et al. Phys. Rev. B **68** (2003) 140101(R).
3) S. Marchesini et al. Optics Express **11**(2003), 2344.
4) M. R. Howells et al.: to be published in J. Elect. Spect. Rel. Phen. (2005)
5) H. N. Chapman et al.: submitted (2005) arXiv:physics/0509066
6) S. Marchesini et al: these proceedings (IT23).
7) T. Beetz, et al. Nucl. Instrum. Meth. A **545** (2005) 459.
8) M. R. Howells et al, Proc. SPIE **4783** (2002), 65.
9) D. R. Luke, Inverse Problems **21** (2005), 37.
10) D. Shapiro et al.: to be published in Proc. Nat. Acad. Sci. (2005).
11) J. R. Fienup, J. Opt. Soc. Am A **36** (1997), 8352.
12) C. Giacovazzo et al *Fundamentals of Crystallography* (OUP, 2002), 2nd ed., p. 739.